

# The experimental research of piezoelectric actuator with two vectors of polarization direction

R. Lučinskis\*, D. Mažeika\*\*, T. Hemsel\*\*\*, R. Bansevicius\*\*\*\*

\*Vilnius Gediminas Technical University, Saulėtekio al. 11, 10223 Vilnius, Lithuania,

E-mail: Raimundas.Lucinskis@fm.vgtu.lt

\*\*Vilnius Gediminas Technical University, Saulėtekio al. 11, 10223 Vilnius, Lithuania,

E-mail: Dalius.Mazeika@fm.vgtu.lt

\*\*\*Paderborn University, Fürstenallee 11, 33102 Paderborn, Germany, E-mail: Tobias.Hemsel@uni-paderborn.de

\*\*\*\*Kaunas University of Technology, Kęstučio 27, 44312 Kaunas, Lithuania, E-mail: Ramutis.Bansevicus@ktu.lt

## 1. Introduction

One of the trends of mechatronics system development is reducing the size of the systems. This feature can be achieved by employing multi-degree of freedom (multi-DOF) piezoelectric actuators [1-7]. Development of multi-DOF actuator is complex engineering problem. Usually two design principles are used to build this type of actuator i.e. complex design of the oscillator is used or specific electrode pattern of piezoelectric transducer is applied. Authors introduce another way to build a multi-DOF actuator that is to use transducer with two vectors of polarization and appropriate pattern of electrodes respectively [1, 7, 8]. Independent oscillations of contact point in three directions can be achieved applying different control schemes of the electrodes.

Several multi-DOF piezoelectric motors are developed till now as well as actuators that have different design and operating principles [6-16]. One of the most frequently used principles is based on superposition of longitudinal and flexural oscillations of a beam. This paper presents study of beam type piezoelectric actuator with two perpendicular vectors of polarization. Applying different excitation schemes of the actuator, 3-DOF movement of the positioned object can be achieved.

## 2. Design of piezoelectric actuator

Introduced beam type piezoelectric is build so that one half of the actuator is polarized towards  $Ox$  axis while another half is polarized towards  $Oy$  axis (Fig. 1, a) [8]. It means that vectors of polarization are perpendicular. The electrodes of each half of the actuator are divided into two sections: one section of the electrode is seamless and designed for excitation of longitudinal oscillations while the other section is divided into two equal units along actuator's axis and is used for excitation of the flexural oscillations. The length of the seamless section is equal to 1/6 of piezoactuator length whereas the length of divided section is equal to 1/3 of piezoactuator length. The excited and grounded electrodes are divided symmetrically.

In order to excite flexural oscillations in desirable plane one of the sections of divided electrodes and both seamless electrodes are excited. For example oscillations in  $yOz$  plane are achieved when electrode No. 1, No. 5 and No. 6 (Fig. 1, b) are excited. Different phase of oscillation is obtained depending on the selected electrode (No. 1 or No. 2). This type of electrode excitation allows achieving

reverse motion of the elliptical motion. The similar principle is used to excite flexural oscillation in  $xOz$  plane (Fig. 1, c). To perform rotational movement of the slider the electrodes No. 1, No. 3, No. 5 and No. 6 are excited (Fig. 1, d). 3-DOF movements of the slider can be achieved combining different electrodes into various excitation schemes.

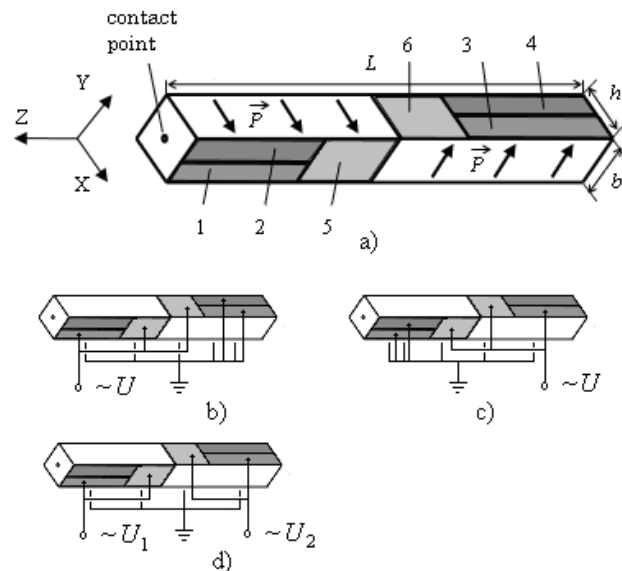


Fig. 1 Piezoelectric actuator with two vectors of polarization: a - principal scheme of the actuator and placing of the electrodes; b - the actuator's excitation scheme No.1; c - the actuator's excitation scheme No.2; d - the actuator's excitation scheme No.3

## 3. Numerical modeling with FEM

ANSYS v.11 software was used for numerical modeling and simulation. Finite element model (FEM) was made of SOLID5 finite elements [17]. It was assumed in the model that piezoactuator is monolithic and has ideal polarization. The SP6 piezoceramics was used for the modeling. The following dimensions of piezoactuator model were used  $b = h = 4.6$  mm and  $L = 46$  mm (Fig. 1). No mechanical constrains were applied in the model. Electrodes were created by grouping surface nodes of the FEM model and harmonic voltage of excitation  $U = 100$  V was applied. The grounding voltage was set to 0 V.

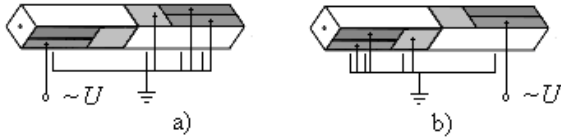


Fig. 2 The excitation schemes of piezoelectric actuator used for experiment: a - 1st case of the actuator's excitation; b - 2nd case of the actuator's excitation

The two excitation cases were used for numerical simulation and experimental study (Fig. 2, a, b). 1st case of excitation: the electrode No.1 is excited and oscillations in the  $xOz$  plane are expected. 2nd case of excitation is when the electrode No. 3 is excited and oscillations in the  $yOz$  plane are expected.

Modal shapes and resonant frequencies of the actuator were calculated. Harmonic response analysis of the actuator was done when the excitation frequency has range from 0 kHz to 100 kHz with 100 Hz frequency step. The 1st scheme was used for excitation (Fig. 1, b). The oscillations of the piezoactuator contact point were analyzed. It has elliptical type trajectory during one period of the oscillation.

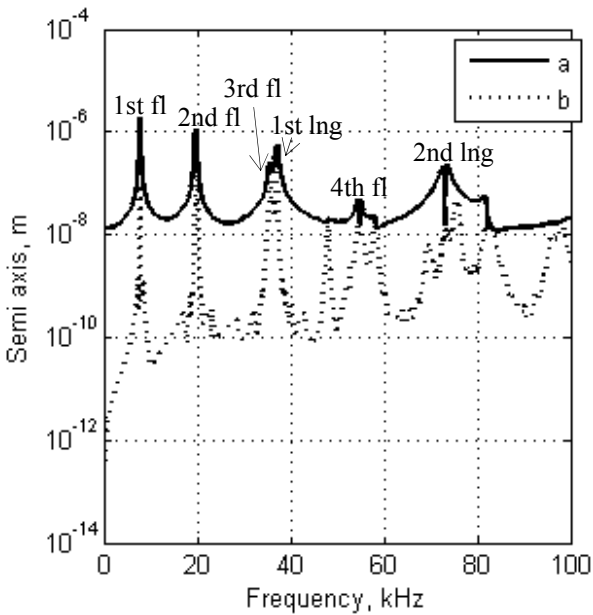


Fig. 3 Dependence of the length of major and minor semi-axes of elliptical trajectory of actuator contact point on excitation frequency

Fig. 3 shows the dependence of the length of major and minor semi-axes of elliptical motion of the actuator contact point from the excitation frequency. Peaks can be noticed in the graphs where the first three peaks represent 1st, 2nd and 3rd flexural modes and the fourth peak corresponds to 1st longitudinal resonance oscillations.

The detailed list of resonance frequencies and corresponding modes of oscillation is given in Table 1. Oscillation trajectories of contact point will be analyzed in more detail when 2nd and 3rd flexural and 1st longitudinal resonance frequencies are applied to electrodes of the actuator.

Trajectories of contact point movement are presented in Fig. 4 and Fig. 5 when the actuator is excited applying 1st and 2nd schemes at 2nd flexural resonance

Table 1

Oscillation modes of the piezoelectric actuator

Mode type	Frequency, Hz
1st flexural	7400
2nd flexural	19300
3rd flexural	35400
1st longitudinal	36800
1st lexural	54200
2nd longitudinal	73400

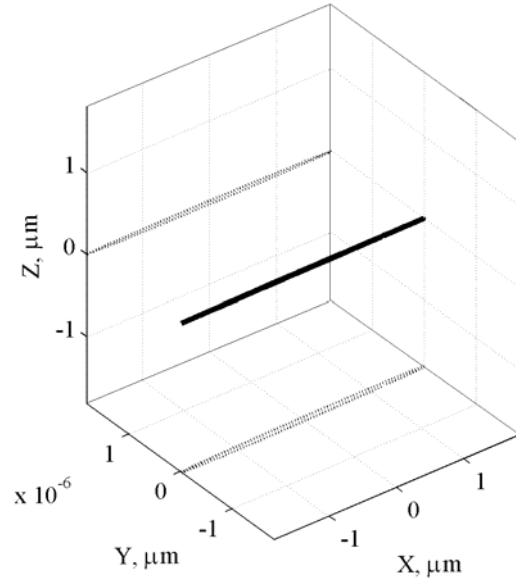


Fig. 4 Trajectory of the actuator's contact point obtained when exciting scheme No.1 is used (19300 Hz)

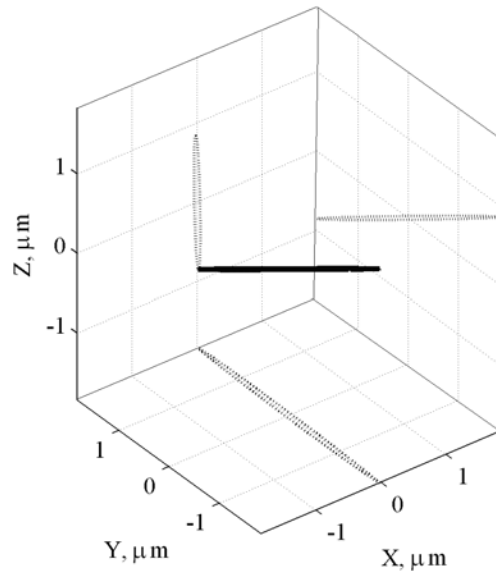


Fig. 5 Trajectory of actuator contact point while exciting scheme No.2 is used (19300 Hz)

frequency. Major axis of elliptical trajectory of the contact point is parallel to  $x$  and  $y$  axis when 1st and 2nd excitation point is parallel to  $x$  and  $y$  axis when 1st and 2nd excitation schemes are used respectively. By observing these two ellipses it can be noticed that the trajectory presented in Fig. 5 has larger  $z$  direction component. This can be explained in the way that when scheme No.1 is used the contact point is in a distance of 2/3 actuator length from the excited electrode meanwhile when 2nd excitation scheme

is used, the contact point is next to the electrode. Different component of  $z$  axis is obtained because of different location of contact point to the electrode.

Oscillation trajectories of the contact point obtained at the excitation frequency equal to 35400 Hz are given in Figs. 6 and 7 when the 1st and 2nd excitation schemes are used respectively. Analyzing both ellipses it can be seen that projections of the major semiaxis to  $xOy$  plane are similar as were in the case when excitation frequency at 2nd flexural mode was used. The projections reach the angle of approximately  $90^\circ$ . However, there is an important note that the 3rd flexural mode is close to the 1st longitudinal mode. Therefore the major semiaxes of given trajectories have larger components in the direction of  $z$ -axis that represent direction of longitudinal oscillations of the actuator.

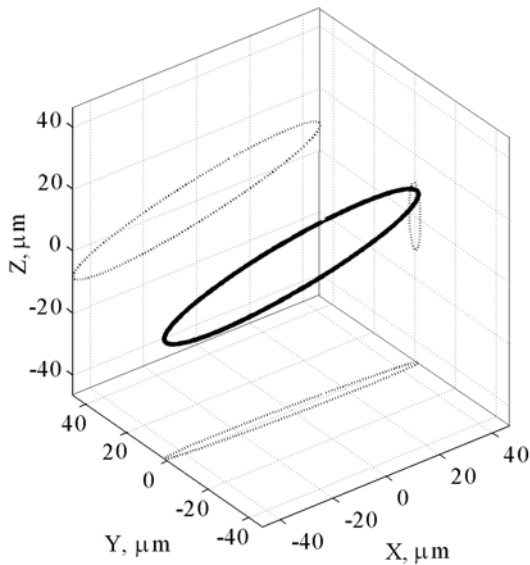


Fig. 6 Trajectory of the actuator's contact point obtained while exciting scheme No.1 is used (35400 Hz)

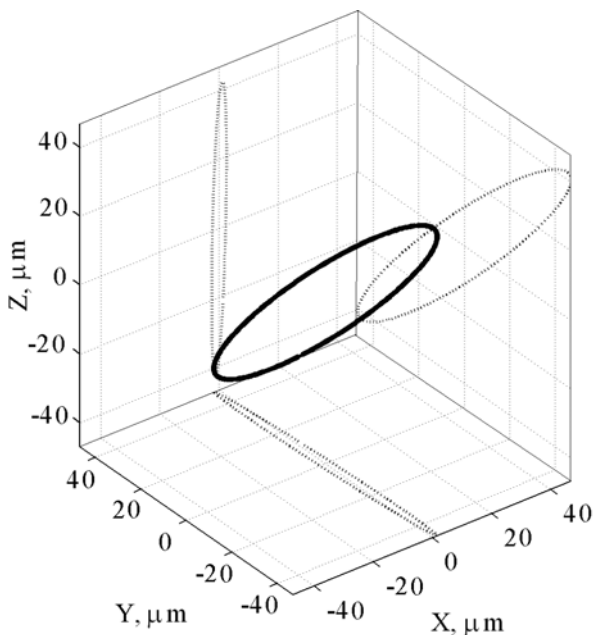


Fig. 7 Trajectory of the actuator's contact point while exciting scheme No. 2 is used (35400 Hz)

Frequency of the 3rd flexural mode does not coincide exactly with the 1st longitudinal mode as it can be

seen from Table 1. So trajectories of contact point motion when excitation frequency is equal to the frequency of the 1st mode of longitudinal oscillation were calculated. The 1st and 2nd excitation schemes were used as in previous cases. Results of calculations are given in Figs. 8 and 9.

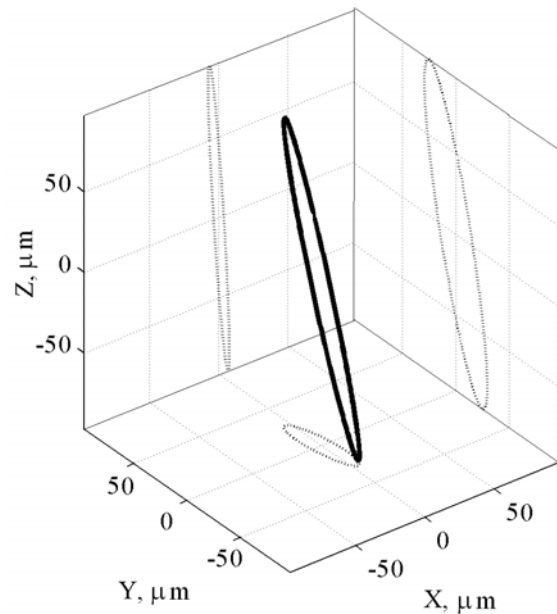


Fig. 8 Trajectory of the actuator's contact point while exciting scheme No. 1 is used (36800 Hz)

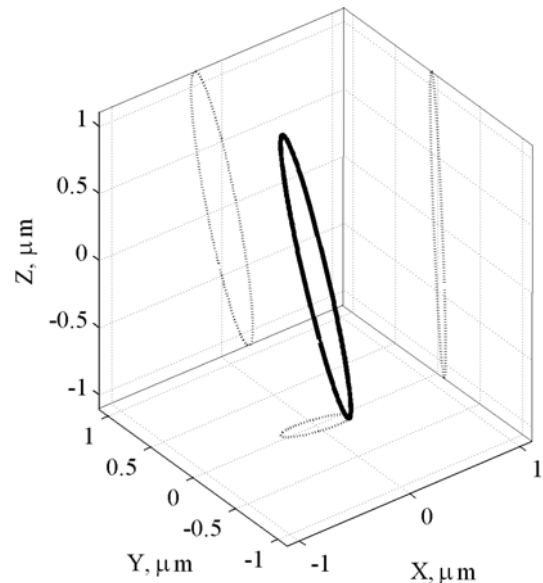


Fig. 9 Trajectory of the actuator's contact point while exciting scheme No.2 is used (36800 Hz)

It can be seen that length of major axes of the ellipses are different because of different excitation schemes. When the electrode is located closer to the contact point (1st scheme) when larger longitudinal vibration amplitude is achieved.

#### 4. Experimental investigation of piezoelectric actuator

Prototype piezoelectric actuator was made for the experimental investigation (Fig. 10). The same excitation schemes were used as in numerical simulation.

The sections of electrodes were created by burning off a silver layer with electric arc. Formation procedure

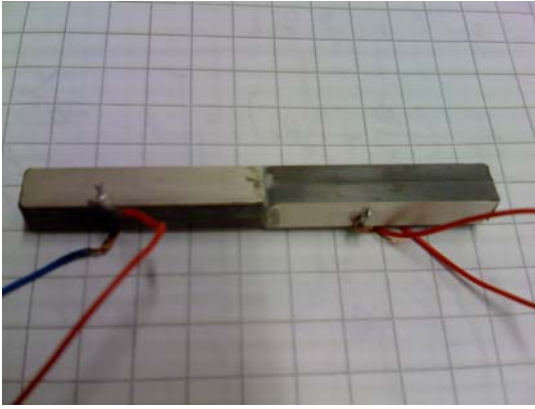


Fig. 10 The experimental model of piezoelectric actuator

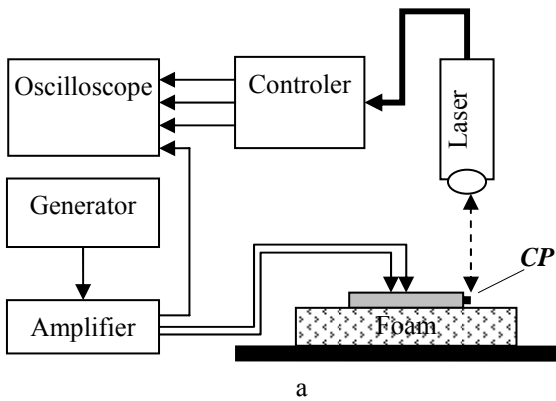


Fig. 11 The principle scheme (a) and photo (b) of the experimental stand

of the electrodes was local and did not change temperature of actuator bulk. So it was assumed that it did not change the quality of piezoelectric material. Special complex measurement stand has been developed for experimental investigation.

The principle scheme and photo of the experimental stand is shown in Fig. 11. The actuator was put on the foam and oscillations were measured. It was assumed that

soft but not viscous layer of the foam will not make influence to the measured oscillations of the actuator.

Generator (Wavetek 395) was used to generate harmonic electrical signal and amplified using amplifier (Bruel&Kjaer 2713). Signal from the amplifier is transferred to the electrodes of the actuator and to an oscilloscope (Yokogawa DL716) as well. This input is needed for the calculation of phase change between the excited and measured signals of oscillations. Oscillations of the actuator contact point are measured by a laser vibrometer (Polytec CLV-3D). Forthcoming and processed signal is sent to a controller (Polytec CLV-3000) which decodes the signal to the oscillation speed component  $v_x$ ,  $v_y$  and  $v_z$  and transfer forthcoming signal to the oscilloscope. The data transferred to the oscilloscope is written and saved for the next step of measurement.

First of all admittance of the actuator has been measured in order to find resonance frequencies. Impedance analyzer (HP 4192A) was employed for the measurement. Fig. 12 shows results of the measured and calculated impedance. By comparing these graphs it can be noticed that measurement result and the results from numerical simulation have good agreement.

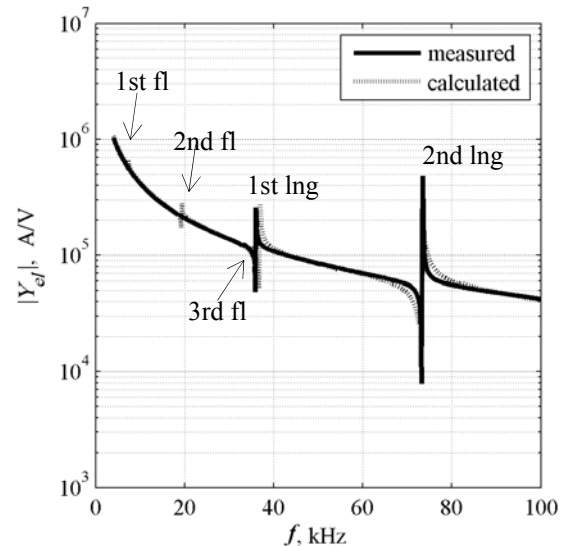


Fig. 12 Admittance of the actuator

Table 2  
Measured resonance frequencies of the actuator

Mode	Frequency, Hz
1st flexural	7050
2nd flexural	18650
3rd flexural	33300
1st longitudinal	35900
2nd longitudinal	73500

Measured frequencies at the peaks of admittance values mostly coincide with the calculated resonance frequencies. The calculated and measured admittance values have small differences but do not exceed 10%. The comprehensive results of the measured impedance data are shown in Table 2 and Figs. 13-15.

By comparing data presented in the Table 1 and Table 2 it can be noticed that measured frequencies are lower than calculated. The biggest difference between the results did not exceed the error of 6%.

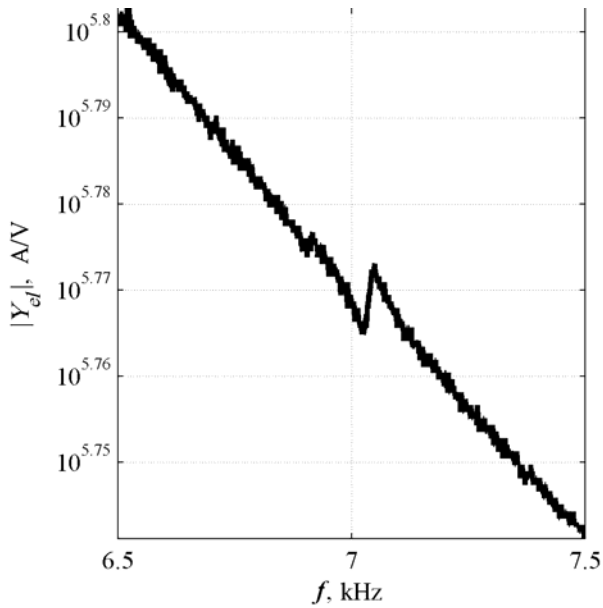


Fig. 13 Measured admittance at the range of *1st* flexural mode

Figs. 12-14 demonstrate the impedance peaks at the frequency close to *1st*, *2nd* and *3rd* flexural modes respectively. Two peaks can be seen in each figure. These peaks represent symmetrical modes of flexural oscillations in two perpendicular directions. From Figs. 12-14 it can be seen that difference between two symmetrical resonant frequencies increases when the mode number of flexural oscillations increases as well. For example difference between the resonances at *2nd* flexural mode is approximately equal to 300 Hz while the difference at the *3rd* flexural mode is equal to 400 Hz.

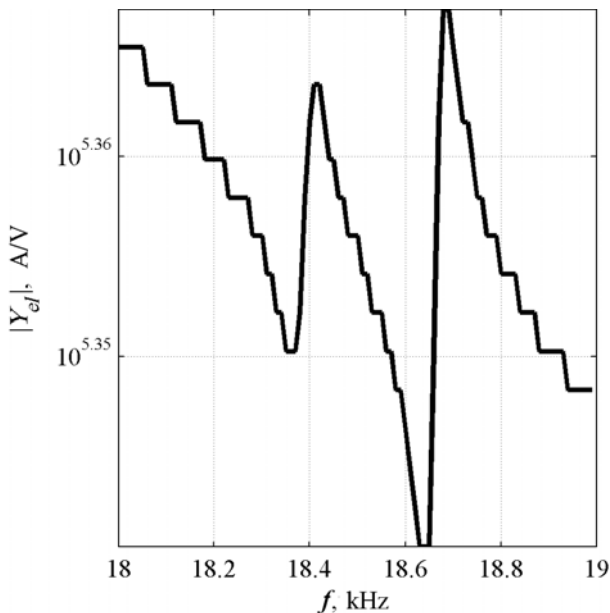


Fig. 14 The measured admittance at the range of *2nd* flexural mode

Measurement of contact point trajectories were done in order to compare it with the trajectories calculated in numerical modeling. All the measurements were done by exciting the actuator with the same excitation voltage 100 V and using the same excitation schemes as was done in numerical simulation. Linear speed components  $v_x$ ,  $v_y$

and  $v_z$  of the contact point were measured with laser vibrometer. Speed values were coded by the voltage amplitudes at the controller output.

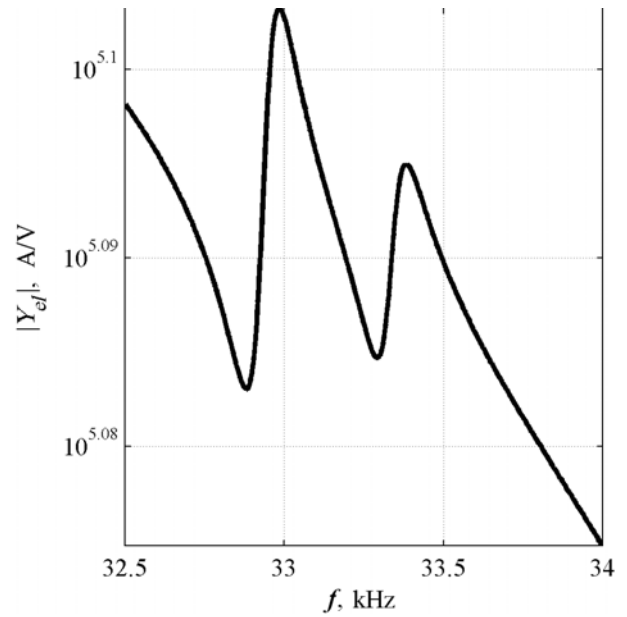


Fig. 15 The measured admittance at the range of *3rd* flexural mode

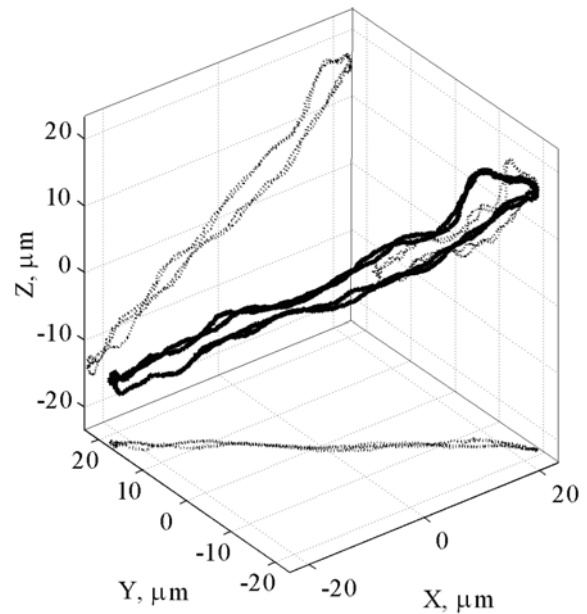


Fig. 16 The trajectory of the contact point when *1st* excitation scheme is used (18700 Hz)

The accuracy of 25 mm/s/V was used during the measurements. The coordinates of the contact point were calculated from the given data. Measured trajectories are shown in Figs. 16-21 where each curve is composed of 1000 measured points.

Figs. 16, 17 show the trajectories when *1st* and *2nd* excitation schemes are applied at the frequency equal to the *2nd* flexural mode. The excitation frequency was set to 18.7 kHz. It can be noticed that parameters of the ellipses differ because of different excitation schemes. Comparing results from numerical modeling (Figs. 4, 5) and experimental investigation it can be seen that they slightly differ because of the influence of two symmetrical flexural modes into measured vibrations of the contact point.

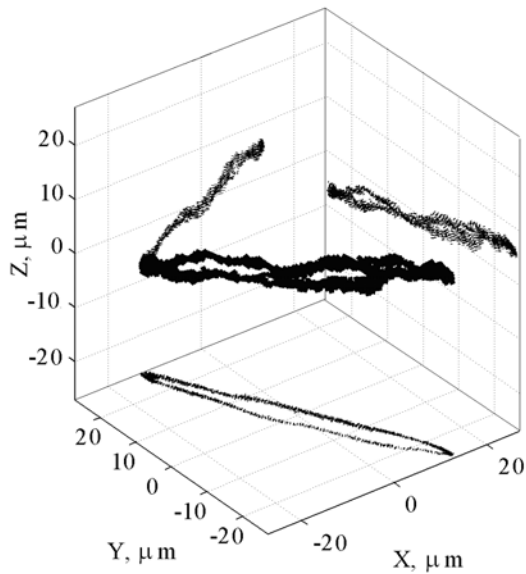


Fig. 17 The trajectory of the contact point when *2nd* excitation scheme is used (18700 Hz)

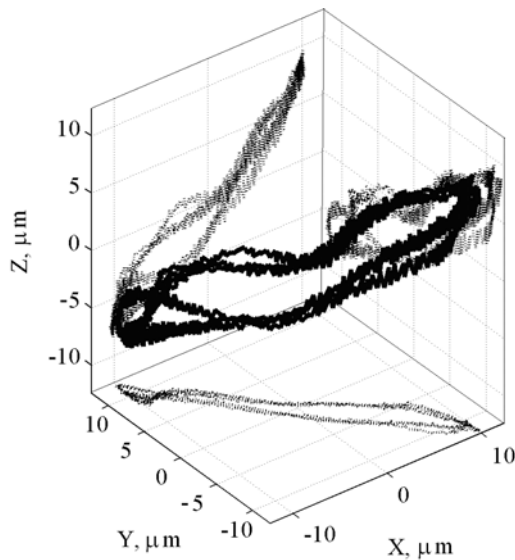


Fig. 18 The trajectory of the contact point when *1st* excitation scheme is used (33200 Hz)

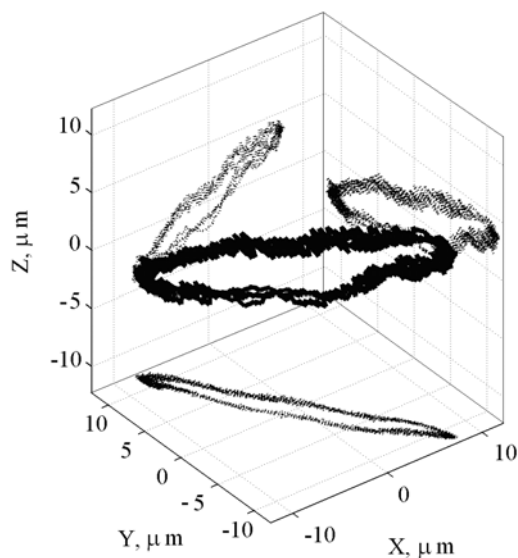


Fig. 19 The trajectory of the contact point when *2nd* excitation scheme is used (33200 Hz)

Figs. 18 and 19 show measured elliptical trajectories of the contact point, when excitation frequency is close to *3rd* flexural mode was used. This frequency closed to *1st* longitudinal mode as well, so vibration components into *z* axis are bigger than in previous cases. It can be seen; parameters of the ellipses in Figs. 18 and 19 weakly depend on excitation schemes. This can be explained as damping influence of the foam on oscillations of the actuator.

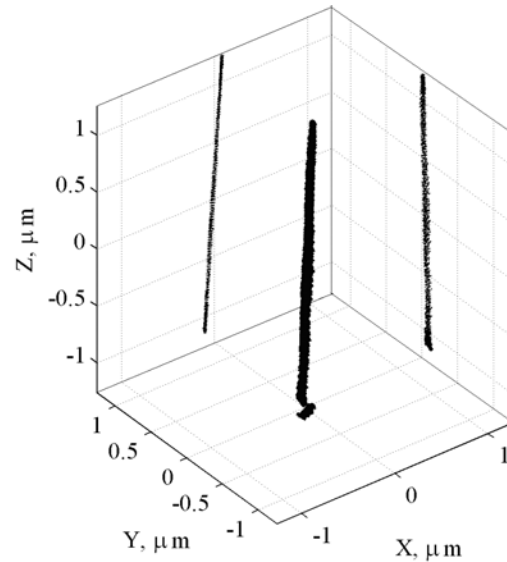


Fig. 20 The trajectory of the contact point when *1st* excitation scheme is used (35500 Hz)

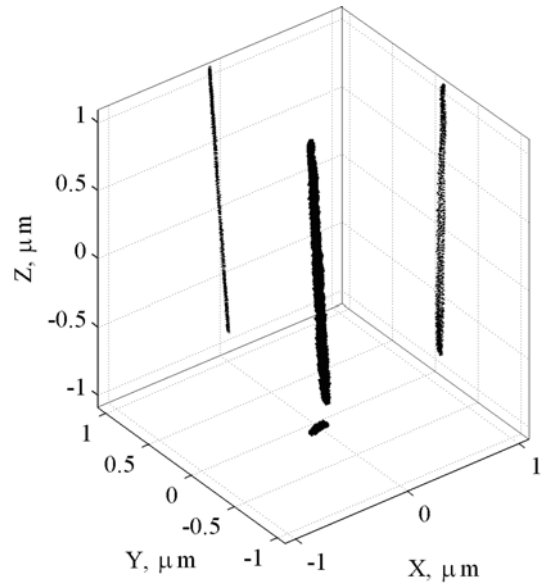


Fig. 21 The trajectory of the contact point when *2nd* excitation scheme is used (35500 Hz)

The last measurement was done when the excitation frequency 35.5 kHz was used. This frequency is very close to *1st* longitudinal resonance, so in this case longitudinal component of the oscillation is considerably larger than others and the contact point moves towards a very spiky elliptical trajectory (Figs. 20 and 21).

## 5. Conclusion

Numerical and experimental investigation of the piezoelectric actuator with two polarization vectors confirm that elliptical trajectory of motion can be achieved in

two perpendicular directions. Parameters and direction of elliptical motion of contact point can be controlled when different excitation schemes are applied. Results of numerical and experimental investigation are in good agreement.

Experimental investigation highlighted the problems with symmetrical flexural modes in the analyzed piezoelectric actuator that had square cross-sectional area. It was clarified that small changes in excitation frequency make considerable influence on orientation and parameters of elliptical motion of the contact point. So in order to obtain more stable trajectory it is recommended to use beam with non square cross-section.

### Acknowledgement

This work has been supported by Lithuanian State Science and Studies Foundation, Project No. B-07017, "PiezoAdapt", Contract No. K-B16/2009-1.

### References

1. **Ragulskis, K., Bansevicius, R., Barauskas, R., Kulvietis, G.** Vibromotors for Precision Microrobots. -New York: Hemisphere Publishing, 1988.-310p.
2. **Fung, R-F., Fan, C-T., Lin, W-C.** Design and analysis of a novel six-degrees-of-freedom precision positioning table. -Proc. IMechE Vol. 223 Part C: J. Mechanical Engineering Science, 2009, p.1203-1212.
3. **Jywel, W., Jeng, Y-R., Liu, C-H. Teng, Y-F., Wu, C-H., Hsieh, T-H., Duan, L-L.** Development of a middle-range six-degrees-of-freedom system. -Proc. IMechE Vol. 224 Part B: J. Engineering Manufacture, 2009, p.1-10.
4. **Limanauskas, L., Nemčiauskas, K., Lendraitis V., Mizarienė, V.** Creation and investigation of nanopositioning systems. -Mechanika. -Kaunas: Technologija, 2008, Nr.3(71), p.62-65.
5. **Rong, W.B., Sun, L.N., Wang, L.F., Qu, D.S.** A precise and concise 6-DOF micromanipulator driven by piezoelectric actuators. -ACTUATOR 2008, 11th International Conference on New Actuators, Bremen, Germany, 9-11 June 2008, p.1022-1025.
6. **Park, S-H., Baker, A., Randall, A.C., Uchino, K., Eitel, R.** Integrated fiber alignment package (IFAPTM) with a compact piezoelectric 2D ultrasonic motor. -ACTUATOR 2008, 11th International Conference on New Actuators, Bremen, Germany, 9-11 June 2008, p.178-183.
7. **Bansevicius, R., Ragulskis, K.** Vibromotors. -Vilnius: Mokslas, 1981.-193p. (in Russian).
8. **Bansevicius, R.,** Latest trends in the development of piezoelectric multi-degree-of-freedom actuators/sensors, responsive systems for active vibration control. -NATO Science Series. -Kluwer, Dordrecht, 2002, p.207-238.
9. **Bansevicius, R., Parkin, R., Jebb, A., Knight, J.** Piezomechanics as a subsystem of mechatronics: present state of the art, problems, future developments. -Industrial Electronics, IEEE Transactions, 1996, v43, issue 1, p.23-29.
10. **Hemsel, T., Mracek, M., Twiefel, J., Vasiljev, P.** Piezoelectric linear motor concepts based on coupling of longitudinal vibrations. -Ultrasonics, 22 December 2006, v. 44, supplement 1, p.591-596.
11. **Stan, S.-D., Balan, R., Maties, V.** Modelling, design and control of 3DOF medical parallel robot. -Mechanika. -Kaunas: Technologija, 2008, Nr. 6(74), p.68-71.
12. **Vasiljev, P., Mazeika, D., Kulvietis, G., Vaiciulienė, S.** Piezoelectric actuator generating 3D-rotations of the sphere. -Solid State Phenomena, vol.13, Mechatronic Systems and Materials. Trans tech Publications, Switzerland, 2006, p.173-178.
13. **Vasiljev, P., Borodinas, S., Bareikis, R., Luchinskis, R.** The square bar-shaped multi-DOF ultrasonic motor. -Journal of Electroceramics, Volume 20, Numbers 3-4 / August, 2008, p.231-235.
14. **Zhao, Ch., Lia, Z., Huang, W.** Optimal design of the stator of a three-DOF ultrasonic motor. -Sensors and Actuators A: Physical, Volume 121, Issue 2, 30 June 2005, p.494-499.
15. **Dembélé, S., Rochdi, K.** A three DOF linear ultrasonic motor for transport and micropositioning. -Sensors and Actuators A: Physical Volume 125, Issue 2, 10 January 2006, p.486-493.
16. **Lucinskis, R., Mazeika, D., Bansevicius, R.,** Modeling and analysis of multi-DOF piezoelectric actuator with two directional polarization. -Proceedings of the 14th International Conference "Mechanika 2009". -Kaunas: Technologija, 2009, p.255-258.
17. ANSYS Release 10.0. Documentation for ANSYS. 2005 SAS IP, Inc.

R. Lučinskis, D. Mažeika, T. Hemsel, R. Bansevicius

EKSPERIMENTINIS DVIEM KRYPTIMIS  
POLIARIZUOTO PJEZOELEKTRINIO KEITIKLIO  
TYRIMAS

R e z i u m ė

Straipsnyje pateikiami dviem kryptimis poliarizuoto piezokeitiklio tyrimo rezultatai. Nagrinėjamas piezokeitiklis yra kvadratinio skerspjūvio strypas, kurio viena ilgio pusė yra poliarizuota statmenai kitai pusei. Abi poliarizacijos kryptys statmenos keitiklio išilginei ašiai. Keitiklio elektrodai padalyti taip, kad užtikrintų lenkimo virpesius, lygiagrečius su viena iš lenkimo ašių, ir galėtų sužadinti pirmąją išilginių virpesių modą. Šis tyrimas parodė, kad tokio tipo konstrukciją turintis keitiklis yra tinkamas trijų laisvės laipsnių slankiklio judesiui formuoti. Pasirinkus atitinkamą elektrodų išsidėstymo atvejį ir atitinkamai juos žadinant galima valdyti kontaktinio taško trajektorijas. Darbe pateikti pjezoelektrinio keitiklio skaitinio modeliavimo ir eksperimentinių tyrimų rezultatai. Jie palyginti pateikiant išvadas ir rekomendacijas dėl tolesnio tokio tipo piezokeitiklio tyrimo.

R. Lucinskis, D. Mazeika, T. Hemsel, R. Bansevicius

THE EXPERIMENTAL RESEARCH OF  
PIEZO-ELECTRIC ACTUATOR WITH TWO  
VECTORS OF POLARIZATION DIRECTION

S u m m a r y

The paper presents results of the investigation of piezoelectric actuator with two different vectors of polarization. The beam type piezoactuator has square cross-section and different half of the actuator has different direction of polarization vector. Both vectors are perpendicular to longitudinal axis of the actuator. The electrodes of each half of the actuator are divided into two sections used for the excitation of longitudinal and flexural oscillations. Applying different excitation schemes of the actuator, 3-DOF movement of the positioned object can be achieved and trajectories of contact point motion can be controlled as well. The results of numerical modeling and experimental investigation are given in the paper. Recommendations for further development of this type actuator are given.

Р. Лучинскис, Д. Мажейка, Т. Гемзель, Р. Бансявичюс

ЭКСПЕРИМЕНТАЛЬНОЕ ИССЛЕДОВАНИЕ  
ПЬЕЗОЭЛЕКТРИЧЕСКОГО ПРЕОБРАЗОВАТЕЛЯ С  
ДВУМЯ ВЕКТОРАМИ НАПРАВЛЕНИЯ  
ПОЛЯРИЗАЦИИ

Р е з ю м е

В этой статье представляются результаты исследований пьезопреобразователя с двумя векторами направления поляризации. Исследуемый преобразователь является стержнем квадратного сечения, одна половина длины которого поляризована в направлении, перпендикулярным направлению поляризации другой половины преобразователя. Электроды преобразователя разбиты на секции таким способом, чтобы возбуждая их, были бы получены поперечные колебания, параллельные одной из осей собственных поперечных колебаний. Цель исследования доказать, что упомянутая конструкция преобразователя является способной формировать движение с 3-мя степенями свободы, а выбрав подходящую топографию расположения электродов и подходящим образом их возбуждая, возможен контроль траекторий контактной точки. В этой статье представляются результаты математического моделирования и экспериментального исследования реальной экспериментальной модели.

Received December 29, 2009

Accepted March 25, 2010

DOI: 10.5755/j02.mech.15521